Available online at www.sciencedirect.com
ScienceDirect
Geochimica et Cosmochimica Acta 71 (2007) 4125–4133
Geochimica et Cosmochimica Acta
www.elsevier.com/locate/gca

# Impact-shock behavior of Mg- and Ca-sulfates and their hydrates

Fuping Zhang [1], Toshimori Sekine *

*National Institute for Materials Science, 1-1 Namiki, Tsukuba 305-0044, Japan*

Received 2 February 2007; accepted in revised form 11 June 2007; available online 29 June 2007

## Abstract

Shock recovery experiments on $MgSO_4$, $CaSO_4$, and their hydrates (kieserite, epsomite, and bassanite) were performed to investigate shock-induced dehydration and decomposition at shock pressures up to 36 GPa. The recovered solid samples indicated dehydration at pressures below 24 GPa, but no clear evidence was found for possible decomposition of $MgSO_4$ and $CaSO_4$ to produce MgO or CaO as final products. These sulfates and hydrates have been observed on the surface of Mars, and the present experimental results can be applied towards understanding the presence of surface water on Mars and the recycling of water by impacts. This finding that the sulfate hydrates undergo dehydration upon impact, as well as the fact that the sulfates $CaSO_4$ and $MgSO_4$ absorb moisture, suggests the total amount of water on Mars has remained almost unchanged since the time of formation of the planet.

## 1. INTRODUCTION

Sulfur on Mars has been recognized since the energy-dispersive X-ray fluorescence spectroscopy element analyses were conducted during the Viking landing mission (Clark et al., 1982). Identification of hydrated sulfates on the surface of Mars (Gellert et al., 2004) and in veins of some meteorites such as the Martian SNC (Shergottite–Nakhlite–Chassignite) meteorites and the CI and CM chondrites (Richardson, 1978; Burgess et al., 1991; Ciesla et al., 2003; Tonui et al., 2003) has drawn considerable attention of researchers toward these sulfate hydrates than in the past. However, there are many reports that maintain that the hydrates in meteorite veins are more likely terrestrial origin (e.g. Gounelle and Zolensky, 2001). The recent spectroscopic observations by the Mars Express OMEGA have identified these hydrates as calcium sulfates (gypsum and bassanite), magnesium sulfates (epsomite, hexahydrite, and kieserite), and others including $Fe^{3+}$-sulfate hydrate (jarosite) at widespread locations (Gendrin et al., 2005; Langevin et al., 2005). Sulfur on Mars may provide information regarding the evolutionary records of the Martian atmosphere and regolith (Farquhar et al., 2000), and there is lots of supporting evidence to explain the impact origin of Martian sediments (Knauth et al., 2005) through the discovery made by Mars Exploration Rover Opportunity.

On the other hand, one of the major extinctions on Earth at 65 Ma, first proposed by Alvarez et al. (1980) and to date accepted widely, appears to be related to the impact of a large bolide at Chicxulub, Mexico. The subsequent climatic changes on Earth, resulting in global cooling, are suggested to have been induced by a mechanism that involves impact-induced release of $SO_2$ that caused severe shielding from sunlight. These sulfur-bearing gases are more damaging than the $CO_2$ released from shock-induced degassing of carbonates (Brett, 1992; Sigurdsson et al., 1992; Pope et al., 1997; Pierazzo et al., 2001; Ivanov et al., 2002; Langenhorst et al., 2003). Furthermore, CI and CM chondrites that contain sulfur-bearing minerals, are considered to be primitive according to their geochemistry and their similarity to the solar photosphere and presumably the early solar nebula (Leshin et al., 1997; Ciesla et al., 2003). Therefore, we need to understand how the sulfates and their hydrates are affected when subjected to impact.

---

* Corresponding author.
*E-mail address:* sekine.toshimori@nims.go.jp (T. Sekine).

[1] Present address: Institute of Fluid Physics, Mianyang, Sichuan 621900, PR China.

0016-7037/$ - see front matter © 2007 Elsevier Ltd. All rights reserved.
doi:10.1016/j.gca.2007.06.037

Previous experimental studies on these hydrous sulfates have revealed the occurrence of dehydration on heating. Based on structural characterization, gypsum $CaSO_4·2H_2O$ starts to dehydrate to bassanite $CaSO_4·0.5H_2O$ at 330 K, and the process of dehydration is completed by 374 K at one atmosphere (Abriel et al., 1990). The dehydration temperature increases slightly with increasing pressure at a rate of about 125 K/GPa (McConnell et al., 1987). Heating of bassanite at 373–383 K produces $\gamma$-$CaSO_4$ (Abriel et al., 1990), which is in a metastable phase and rehydrates rapidly at normal atmospheric conditions. Two phase transitions occur at high temperatures: transition to $\beta$-$CaSO_4$ above 525 K and transition to $\alpha$-$CaSO_4$ at about 1470 K; The melting temperature of $CaSO_4$ is 1723 K (Rowe et al., 1967).

There have been several experimental studies done on shocked anhydrite to simulate the Cretaceous/Tertiary (K/T) boundary event. Through shock recovery experiments Chen et al. (1994) investigated the amount of $SO_2$ produced from the reaction of $CaSO_4$ and $SiO_2$, and studied the devolatilization of anhydrite at shock pressures up to 42 GPa. Thermodynamic considerations of shock-induced vaporization have been employed to estimate vapor products from anhydrite (Yang and Ahrens, 1998; Gupta et al., 2001). However, optical microscopic studies, scanning electron microprobe (SEM) examinations, and X-ray diffraction (XRD) studies of shock-loaded anhydrite at pressures up to 64 GPa (Skála et al., 2005) have not indicated any decomposition products. Based on the Hugoniot data on anhydrite and gypsum (Simakov et al., 1974), there seems to be a phase transition at ~25 GPa for gypsum, but no phase transition for anhydrite up to 100 GPa. XRD spectra for shocked anhydrite showed a slight variation of the lattice constant with a maximum variation around a peak shock pressure of 40 GPa, but these patterns were always the same as that for the unshocked sample ($\beta$-form of anhydrite) (Skála et al., 2005).

Magnesium sulfates are known to exist as a series of hydrate forms with various water contents. Among them, only three hydrous phases are stable at normal atmospheric conditions, namely kieserite $MgSO_4·H_2O$, hexahydrite $MgSO_4·6H_2O$, and epsomite $MgSO_4·7H_2O$. All of these are sensitive to humidity and temperature. Their crystal structures have been determined by Hawthorne et al. (1987), Zalkin et al. (1964), and Calleri et al. (1984), respectively. Experimental studies on phase equilibria in the system $MgSO_4$–$H_2O$ were performed by Chou and Seal (2003) for epsomite–hexahydrite at 0.1 MPa and also by Vaniman et al. (2004), Chipera and Vaniman (2007), and Vaniman and Chipera (2006) under conditions similar to those at the Mars surface. According to the experimental results, epsomite converts to hexahydrite by loss of water, and the reversible hydration occurs at 298 K at a relative humidity of ~50%. Kieserite is more stable at higher temperature and survives up to ~670 K. Hexahydrite becomes amorphous—metastably—at 298 K. Heating of the hydrous sulfate produces the final product of $MgSO_4$ which then starts to decompose at 1168 K. It appears that a phase transition from the $\beta$ (low temperature) form to the $\alpha$ (high temperature) form takes place at a temperature close to the melting point (1409 K) (Rowe et al., 1967). However, the system $MgSO_4$–$H_2O$ is strongly metastable and characterized by sluggish kinetics and reaction routes, and exhibits experimental difficulties.

We have investigated a series of dehydration reactions and decompositions on the recovered solids from shocked calcium and magnesium sulfate hydrates. Our aim is to investigate shock-induced dehydration and transformation in the systems $CaSO_4$–$H_2O$ and $MgSO_4$–$H_2O$, but not to determine the phase equilibria. These data will provide valuable information for understanding the impact effects on the surface materials and on the atmosphere of Mars, also in terms of the climate change at the time of the K/T boundary event.

## 2. EXPERIMENTAL

The samples selected were $CaSO_4·0.5H_2O$, $MgSO_4$, $MgSO_4·H_2O$, and $MgSO_4·7H_2O$. The samples other than $MgSO_4·H_2O$ were obtained from Kojundo Chemical Laboratory Co. Ltd, Japan, with a high purity (99%). $MgSO_4·H_2O$ was prepared by heating $MgSO_4·7H_2O$ at 120 °C for 4 days and the composition of the reaction product was confirmed by X-ray diffraction as the single phase of kieserite. Each powder was pressed to a disk (18 mm diameter × ~1 mm thick) in a steel container (30 mm diameter × 30 mm long), at pressures up to 0.5 GPa. The sample was placed at a depth of 3 mm from the impact surface of the container. The apparent densities of the pressed samples were calculated by measuring their thicknesses using a vernier caliper with a margin of error of ~10% (Table 1). The porosity of the sample was also calculated and found to be about 30–50% for $MgSO_4$ and $MgSO_4·H_2O$, about 10–30% for $CaSO_4·0.5H_2O$, and almost zero for $MgSO_4·7H_2O$. Shock recovery experiments were conducted using a 30-mm bore propellant gun (Sekine, 1997). A 3-mm thick steel flyer plate, attached to the head of a projectile, impacted the container. Velocity just before impact was measured with a magnetoflyer method (Kondo et al., 1977).

After successful recovery the containers were cut open to take the samples out. Some of the containers were found to be broken due to sudden formation of gas in the container during pressure release, and no sample was obtained from such shots. The samples thus obtained were investigated immediately by X-ray diffraction (XRD) (Rigake RINT 2200 V/pc Diffractometer, operated at 40 kV, 50 mA with Cu target) in order to identify phases present in the shock-recovered samples at room temperature. The XRD spectra were checked against the database PDF2 of the International Center for Diffraction Data (ICDD). The reference data used in the present study are summarized in Table 2. We also have saved samples in vinyl bags with sealing zippers at ambient condition and measured some of the samples by XRD in order to check the effect of humidity in storage.

The peak shock pressure was calculated by the impedance match method assuming the sample pressure reached equilibrium with the container pressure. The actual pressure experienced by a sample increases stepwise from the

Table 1
Shock-recovery experimental conditions of bassanite ($CaSO_4 \cdot 0.5H_2O$), $MgSO_4$, hexahydrite ($MgSO_4 \cdot H_2O$), and epsomite ($MgSO_4 \cdot 7H_2O$) in steel containers

| Shot No. | Starting material | Initial density ($g/cm^3$) | Sample thickness (mm) | Impact velocity (km/s) | First Pressure (GPa) | Peak pressure (GPa) | Phases identified | Relative XRD peak height ratio |
|---|---|---|---|---|---|---|---|---|
| 1304 | A | 1.88 | 1.10 | 0.667 | <6.2 | 13.4 | A | |
| 1288 | | 1.91 | 1.10 | 0.798 | <7.5 | 16.3 | B + A | B/A :7.1 |
| 1290 | | 1.95 | 1.10 | 1.133 | <11.1 | 24.2 | B | |
| 1294 | | 1.93 | 1.15 | 1.181 | <11.8 | 25.4 | No | |
| 1305 | | 2.39 | 1.05 | 1.190 | <11.9 | 25.7 | No | |
| 1285 | | 2.04 | 1.25 | 1.300 | <13.3 | 28.5 | No | |
| 1307 | C | 1.55 | 1.35 | 0.617 | | 12.3 | E + D | |
| 1286 | | 1.62 | 1.35 | 0.822 | | 16.8 | D + C | D/C: 1.8 |
| 1306 | | 1.59 | 1.30 | 1.000 | | 21.0 | D + C | 1.3 |
| 1292 | | 1.90 | 1.20 | 1.159 | | 24.9 | C + D | 0.1 |
| 1283 | | 2.02 | 1.30 | 1.300 | | 28.5 | C + D | 0.2 |
| 1291 | | 2.03 | 1.30 | 1.479 | | 33.2 | D + C | 1.1 |
| 1303 | | 1.567 | 1.4 | 1.579 | | 35.9 | C + D | 0.6 |
| 1316 | F | 1.55 | 1.25 | 1.020 | | 21.5 | F + D | |
| 1317 | | 1.46 | 1.20 | 1.010 | | 21.3 | F + D + C | |
| 1319 | | 1.54 | 1.15 | 1.090 | | 23.2 | F + C + D | |
| 1318 | | 1.60 | 1.20 | 1.100 | | 23.4 | No | |
| 1287 | G | 1.63 | 1.20 | 0.822 | | 16.8 | G + D | D/G: 0.2 |
| 1301 | | 1.51 | 1.15 | 0.900 | | 18.6 | G + D | 0.9 |
| 1302 | | 1.78 | 1.05 | 0.900 | | 18.6 | G + D | 0.4 |
| 1289 | | 1.81 | 1.10 | 1.149 | | 24.6 | G + D | 0.1 |
| 1308 | | 1.50 | 1.20 | 1.160 | | 24.9 | D + G | 2.7 |
| 1322 | | 1.78 | 0.54 | 1.176 | | 25.3 | D + G | 1.9 |
| 1323 | | 1.78 | 0.54 | 1.278 | | 27.9 | D + G | 5.2 |
| 1293 | | 1.74 | 1.05 | 1.159 | | 24.9 | No | |
| 1284 | | 1.72 | 1.24 | 1.300 | | 28.5 | No | |

*Note*. A, $CaSO_4 \cdot 0.5H_2O$; B, β-$CaSO_4$; C, β-$MgSO_4$; D, $MgSO_4 \cdot 6H_2O$; E, α-$MgSO_4$; F, $MgSO_4 \cdot H_2O$; G, $MgSO_4 \cdot 7H_2O$; No, no sample remained due to container destruction.

Table 2
Water content, density and the data base for sulfates and their hydrates used in the present study

| Phases | Calculated $H_2O$ (wt%) | Density (g/cm$^3$) | ICDD PDF2[a] numbers | |
|---|---|---|---|---|
| β-$CaSO_4$ | 0 | 2.96 | 01-070-0909 | 00-037-1496 |
| $CaSO_4 \cdot 0.5H_2O$ | 6.21 | 2.75 | | 00-041-224 |
| $MgSO_4 \cdot 7H_2O$ | 51.2 | 1.68 | 01-075-0673 | 00-036-419 |
| $MgSO_4 \cdot 6H_2O$ | 47.4 | 1.72 | 01-072-1068 | 00-024-719 |
| $MgSO_4 \cdot H_2O$ | 13.0 | 2.59 | 01-080-0545 | 00-033-882 |
| β-$MgSO_4$ | 0 | 2.93 | 01-074-1364 | 00-021-546 |
| α-$MgSO_4$ | 0 | — | 01-072-1259 | 00-019-772 |

[a] ICDD PDF2: International Center for Diffraction Data PDF2 plus database.

first shock state to the final peak pressure and decreases adiabatically after about 1 μs. The details of the experimental conditions are given in Table 1. The maximum shock pressure at the first state, corresponding to the incident shock pressure within the dense sample without porosity, was also calculated by the impedance match method where the Hugoniot data for a sample were available. The Hugoniot data for $CaSO_4$ and $CaSO_4 \cdot 2H_2O$ were determined by Simakov et al. (1974). The Hugoniot equation of state for $CaSO_4 \cdot 0.5H_2O$ was calculated for a mixture of 3 mol $CaSO_4$ and 1 mol $CaSO_4 \cdot 2H_2O$, while neglecting the temperature difference. The calculated relationship between shock velocity $U_s$ and particle velocity $U_p$ is approximated as $U_s$ (km/s) = 3.52 + 1.57$U_p$ (km/s). Due to the unavailability of Hugoniot data for magnesium sulfate and its hydrates, we were not able to estimate the initial shock pressure. There are inevitable problems related to the physical difference in shock compression processes that can exist between experiments and natural impact phenomena, especially in the case of residual temperature and compression duration (Tomeoka et al., 1999; DeCarli et al., 2002).

Simultaneous differential thermal analysis and thermogravimetric analysis (DTA/TG) were carried out using a Shimadzu DTG-60H instrument, up to a temperature of 1475 K for the starting material of epsomite and two samples of 1286 and 1308. The analyses were done in a nitrogen gas flow (50 ml/min) and at two heating rates of 2–400 °C/min and 10–1200 °C/min as separate measurements for 5–10 mg samples. The results were compared with those reported by Paulik et al. (1981) and Bonello et al. (2005).

## 3. RESULTS

Fig. 1 shows the XRD spectra for $CaSO_4 \cdot 0.5H_2O$ and the shock-recovered samples. The sample shocked at 13.4 GPa (Fig. 1b) shows little difference from the starting material. When the pressure increased to 16.3 GPa, the anhydrous phase (β-$CaSO_4$), as marked by the open circles in Fig. 1d, is a major phase (Fig. 1b). When the pressure reached 24.2 GPa (Fig. 1c), it was found that $CaSO_4 \cdot 0.5H_2O$ completely transformed to anhydrite. Further increase in pressure led to unsuccessful recovery of samples even when much denser samples were shocked to reduce the temperature rise. The shock compression of $CaSO_4 \cdot 0.5H_2O$ caused the incipient dehydration at about 15 GPa and the reaction was completed at 24 GPa.

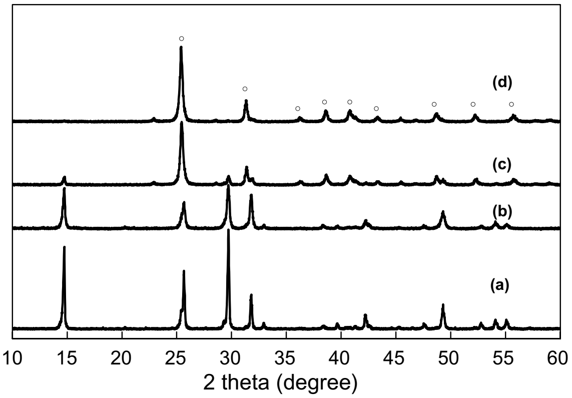

Fig. 1. XRD patterns obtained for bassanite $CaSO_4 \cdot 0.5H_2O$. (a) Starting material, (b) 13.4 GPa sample (#1304), (c) 16.3 GPa sample (#1288), and (d) 24.2 GPa sample (#1290). Open circle, β-$CaSO_4$.

The XRD patterns for $MgSO_4$ and its shocked samples are shown in Fig. 2. All the samples up to 36 GPa were recovered successfully. The XRD peaks for hexahydrite ($MgSO_4 \cdot 6H_2O$) were always observed as in the starting material (β-$MgSO_4$). The amounts of observed hexahydrite varied and there appeared no systematic changes in terms of pressure and initial density, as shown in Fig. 2. All samples were stored in vinyl bags with sealing zippers. The XRD reinvestigation of sample #1306 after 20 days and of sample #1283 after 40 days revealed significant increases in the intensity of hexahydrite peaks and showed a relative decrease in the intensity of peaks of $MgSO_4$, but no other phase seemed to have appeared. The sample shocked at 12.3 GPa indicated the presence of α-$MgSO_4$ (high-temperature form) instead of β-$MgSO_4$. The phase transition from the low temperature form (β-$MgSO_4$) to the high temperature form (α-$MgSO_4$) occurs at 1090 °C and at ambient pressure (Rowe et al., 1967). Under the given shock condi-

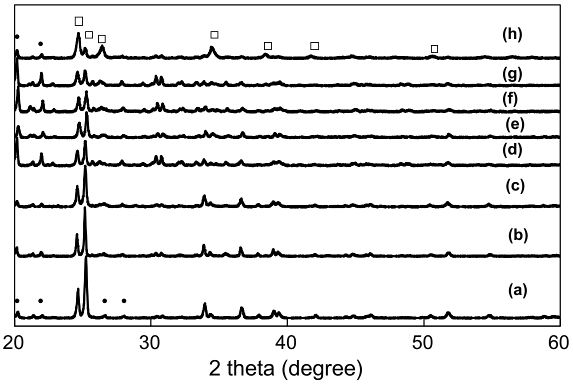

Fig. 2. XRD patterns obtained for magnesium sulfate $MgSO_4$. (a) Starting material, (b) 28.5 GPa sample (#1283), (c) 24.9 GPa sample (#1292), (d) 33.2 GPa sample (#1291), (e) 35.9 GPa sample (#1303), (f) 21.0 GPa sample (#1306), (g) 16.8 GPa sample (#1286), and (h) 12.3 GPa sample (#1307). Solid circle, $MgSO_4 \cdot 6H_2O$ and open square, α-$MgSO_4$.

tions, $MgSO_4$ was found stable and did not decompose up to 36 GPa.

The XRD results for shocked kieserite are shown and compared with those of the starting material in Fig. 3. They always showed the coexistence of kieserite and hexahydrite and showed increasing amounts of β-$MgSO_4$ with increasing shock pressure up to 23.2 GPa. Above this pressure, no sample remained in the container (Table 1). The XRD investigation of kieserite kept in air for three days revealed the formation of hexahydrite, and the coexisting hexahydrite is considered to have formed by the effect of humidity in air. Kieserite appeared to be stable up to a shock pressure of 21–23 GPa, and it rapidly dehydrated above this pressure.

The XRD results for epsomite and its shocked samples are shown in Fig. 4. Hexahydrite was always identified together with epsomite. The *d*-values of the highest XRD peaks for hexahydrite and epsomite were at ~0.44 and ~0.42 nm, respectively, and there were large variations in the relative peak intensities for the two phases. In order to estimate the relative amounts, the height ratio of the highest peaks was calculated (Table 1). The ratio increased with increasing shock pressure and with decreasing initial density. For example, at similar initial densities in shots 1302, 1322, and 1323, the peak height ratios were 0.4, 1.9, and 5.2. At similar shock pressures of 19 GPa in shots 1301 and 1302 and of 25 GPa in shots 1308, 1289, and 1322, the ratios increased with decreasing initial density. It is noteworthy that samples were successfully recovered in containers when smaller amounts of samples were subjected to similar shock pressures in shots 1322 and 1323.

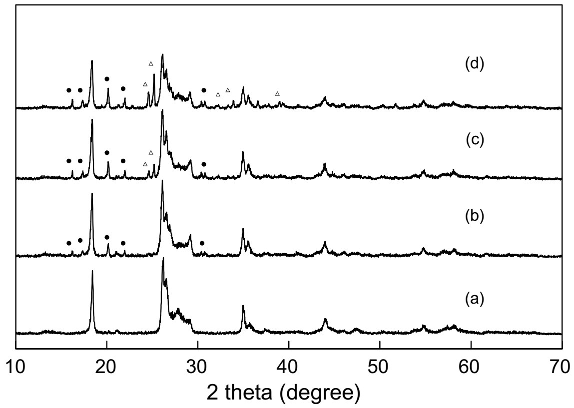

Fig. 3. XRD patterns for kieserite $MgSO_4{\cdot}H_2O$. (a) Starting material prepared by heating epsomite at 120 °C, (b) 21.5 GPa (#1316), (c) 21.3 GPa sample (#1317), and (d) 23.2 GPa sample (#1319). Solid circle, $MgSO_4{\cdot}6H_2O$ and open triangle, β-$MgSO_4$.

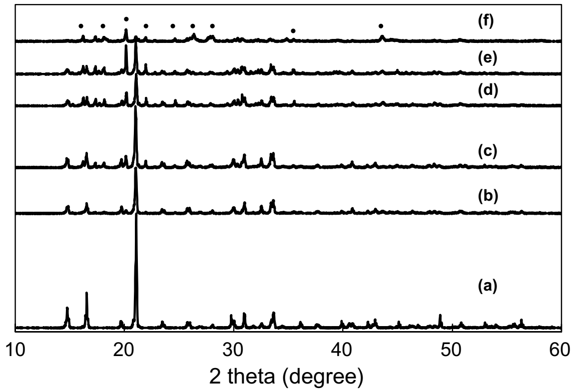

Fig. 4. XRD patterns for epsomite $MgSO_4{\cdot}7H_2O$. (a) Starting material, (b) 24.6 GPa sample (#1289), (c) 16.8 GPa sample (#1287), (d) 18.6 GPa sample (#1302), (e) 18.6 GPa sample (#1301), and (f) 24.9 GPa sample (#1308). Solid circle, $MgSO_4{\cdot}6H_2O$.

DTA/TG analytical results of our starting epsomite up to a temperature of 400 °C are summarized as follows. At a slow heating rate (2 °C/min), there were three endothermic peaks that were seen at 41 °C, at 50 °C (small peak) and at 72 °C (large peak), and one exothermic peak at 270 °C. The TG weight change at 380 °C was 48 wt%. This is compared with the theoretical value of 51 wt% loss after the complete dehydration of epsomite to $MgSO_4$ above 300 °C (Bonello et al., 2005). The TG weight loss was 43.4 wt% before the exothermic peak at 270 °C, and it is very close to the theoretical estimation for dehydration of epsomite into kieserite (43.9 wt%). The TG curve below 100 °C did not show any plateau and the detailed profile for dehydrations from epsomite to kieserite were not clearly observed in the present study. At a high heating rate (10 °C/min), the endothermic peak and the exothermic peak, corresponding to the 72 and 270 °C peaks observed at the low heating rate, shifted to 98.5 and 298 °C, respectively. The DTA/TG curves were flat over the temperature range of 300–800 °C, and an endothermic peak at 1007 °C was observed that corresponds to the decomposition of $MgSO_4$ to MgO plus gas phase. The final weight loss reached 82.3% around 1100 °C. The DTA/TG profiles for samples 1286 and 1308 were essentially the same as that for epsomite, although they contained hexahydrite as the major phase. The weight changes at 380 °C were 43.7% for sample 1286 and 31.4% for sample 1308, and the weight changes at 1100 °C were 81.4% for sample 1286 and 64.5% for sample 1308, respectively. There was an endothermic peak at 327 °C (at 2 °C/min) or 355 °C (at 10 °C/min) that was not observed in the measurements of sample 1308 and epsomite. We do not understand what this peak means.

## 4. DISCUSSION

Initial density of a sample has been found to be an important factor to control the shock dehydration reaction, as well as peak shock pressures, because it is directly related to shock temperature rise. Shock temperature is calculated on the thermodynamic consideration using the Hugoniot equation of state. We calculated model cases for bassanite ($CaSO_4{\cdot}0.5H_2O$) and anhydrite ($CaSO_4$), because their specific data and Hugoniot curves are available. The calculated shock temperatures for bassanite are 670 K at 20 GPa and 1035 K at 30 GPa for a Grüneisen parameter of 1, and 790 K at 20 GPa and 1200 K at 30 GPa for a Grüneisen parameter of 2. Those for anhydrite are 635 K at 20 GPa and 970 K at 30 GPa for a Grüneisen parameter of 1, and

735 K at 20 GPa and 1115 K at 30 GPa for a Grüneisen parameter of 2. Considering the porosity effect, the temperatures should be much higher. The heterogeneous distribution of pores in powder samples causes local temperature rise that initiates the dehydration reactions in the shock process. The dehydration products were observed according to the following reactions:

$$\mathrm{CaSO_4 \cdot 0.5H_2O\ (s) = \beta - CaSO_4\ (s) + 0.5H_2O\ (g)} \quad (1)$$

$$\begin{aligned}\mathrm{MgSO_4 \cdot H_2O\ (s)} &= \mathrm{\beta - MgSO_4\ (s) + H_2O\ (g)\ or} \\ &\quad \mathrm{\alpha - MgSO_4\ (s) + H_2O\ (g)} \end{aligned} \quad (2)$$

$$\mathrm{MgSO_4 \cdot 7H_2O\ (s) = MgSO_4 \cdot 6H_2O\ (s) + H_2O\ (g).} \quad (3)$$

At ambient pressure, hexahydrite becomes unstable at high temperatures relative to kieserite (Bonello et al., 2005), but we observed only hexahydrite as the dehydration product of epsomite. According to the observed shock products, shock temperature was estimated to be in the stability field of β-$CaSO_4$ and β-$MgSO_4$, except for shot 1307 that indicated the presence of α-$MgSO_4$. There is no clear evidence for the decomposition and melting of $CaSO_4$ and $MgSO_4$ from the XRD spectra of the recovered samples, and the shock temperatures for the successfully recovered shots were below their decomposition and melting temperatures.

Magnesium sulfate hydrates show a systematic variation in their density–water content (Table 2). Thermodynamically, pressure causes dehydration to increase density in solids. Shock compression results in a lower hydration state of reaction products. The dehydration experiments indicated stepwise dehydration progressively producing less-hydrated forms of magnesium sulfate. Epsomite dehydrates to hexahydrite but not to the hydrous phases with lower water content. This may have been controlled also by the strength of a container. The sample space in a container can hold a limited gas pressure, and the dehydration from epsomite to kieserite was not observed in the present study; this is because such a large amount of water could not be held in our containers. It would be possible for epsomite on the surface of Mars to dehydrate by impacts not only to hexahydrite but also to other hydrous phases with lower water contents, and even to the anhydrous phase, depending on impact conditions, because Mars can be regarded as an open system. These dehydrations would produce water or ice on the surface. However, this may not be correct if a series of dehydration reactions are controlled by the activation energy barriers for dehydration between phases with more than simple removal of water that require significant crystal structure rearrangement. According to the review by Hawthorne et al. (2000), the $SO_4$ tetrahedra are linked to the $Mg(H_2O)_6$ octahedra through H-bonding in epsomite, but there is no $Mg(H_2O)_6$ octahedron in hexahydrite. Kieserite consists of a three-dimensional infinite framework of cross-linked chains of the $SO_4$ tetrahedra and the $Mg(O, H_2O)_6$ octahedra with shared corners and is more stable than other Mg sulfate hydrates. These structural differences may have a considerable effect at low temperatures such as those at the surface of Mars.

The shock-induced dehydrations of epsomite, kieserite, and basanite indicated abrupt water loss at shock pressures of 21–24 GPa, although the onset pressures appear to be much lower depending on the initial porosity. Peak pressures as indicated from Martian meteorites would be in the range of 5–50 GPa (Nyquist et al., 2001; Fritz et al., 2005), and impact-induced dehydrations could be possible on Mars. When these sulfate hydrates are subjected to meteoritic impact on the Mars surface, there would be a threshold impact velocity for dehydration, depending upon what the impactor is. The bulk density of Martian surface materials is about 1.2–2.6 g/cm$^3$ (Christensen and Moore, 1992), and we here assume that the Mars surface consists of a material with Hugoniot equation of state similar to that of gypsum (density = 2.28 g/cm$^3$) or bassanite (2.75 g/cm$^3$) (Fig. 5). The threshold impact velocity for impact-dehydration can be calculated by means of the impedance match method. Possible impactors include water ice, carbonaceous chondrite, ordinary chondrite, iron meteorite, and their mixtures. Their Hugoniots are listed in Table 3. Fig. 5 illustrates a plot of particle velocity ($U_p$)–pressure ($P$) to estimate an impact velocity. Hugoniot relations for them are given by $U_s = C + SU_p$, where $C$ and $S$ are constants (Table 3). The ranges of impact velocity corresponding to a peak shock pressure of 21–24 GPa are 1.9–5.1 km/s, being comparable to or below the escape velocity of Mars (~5 km/s). Therefore, the ejected materials can return back, and accumulate even if they were dehydrated by impact, although the calculations are assuming no reaction between target and impactor.

The present recovery experiments on magnesium sulfate (β-form) have indicated its high stability at least up to a pressure of 36 GPa (the highest in the present study) and at high shock temperatures where the α-form was stable. We did not obtain any evidence for decomposition to MgO and $SO_2$. Previous experimental results on anhydrite $CaSO_4$ and mixtures of anhydrite and quartz powders gave no direct evidence for decomposition up to about 60 GPa (Skála et al., 2005), although Chen et al. (1994) found the formation of iron sulfide in a shocked mixture of anhydrite, quartz, and iron. They believed that devolatilization of

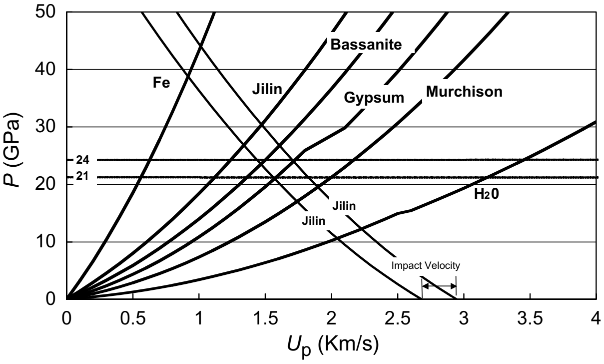

Fig. 5. Pressure ($P$)–particle velocity ($U_p$) plot illustrating the impedance match solution to calculate impact velocity. The shock velocity–particle velocity relations are given in Table 3 for the impactors and targets. The pressure range for the dehydration is 21–24 GPa, and a range of impact velocities for Martian surface of gypsum, impacted by Jilin ordinary chondrite, is shown as an example. See the ranges of impact velocities for various conditions in Table 3.

Table 3
Estimation of critical impact velocities for various bolides to dehydrate sulfate hydrates, approximated by the Hugoniot of gypsum (G) or bassanite (B), at peak pressures of 21–24 GPa. $U_s = C + SU_p$ (both $C$ and $S$ are constants)

| Materials | Density (g/cm$^3$) | $C$ | $S$ | Impact velocity (km/s) | |
|---|---|---|---|---|---|
| | | | | G | B |
| Gypsum (G) | 2.28 | 2.85 | 1.92 ($U_p < 1.8$ km/s) | | |
| | | 2.45 | 1.80 ($U_p > 2.1$ km/s) | | |
| Bassanite (B) | 2.75 | 3.52 | 1.57 | | |
| Murchison | 2.20 | 1.87 | 1.48 | 3.6–3.9 | 3.3–3.6 |
| Jilin | 3.44 | 3.98 | 1.37 | 2.7–2.9 | 2.4–2.7 |
| Iron | 7.85 | 3.93 | 1.58 | 2.1–2.3 | 1.9–2.1 |
| Ice ($H_2O$ ice) | 1.0 | 1.70 | 1.71 ($U_p < 2.5$ km/s) | 4.7–5.1 | 4.5–4.9 |
| | | 2.65 | 1.27 ($U_p > 2.5$ km/s) | | |

Hugoniot data: gypsum from Simakov et al. (1974), bassanite from data estimated in this paper, Murchison from Anderson and Ahrens (1998), Jilin from Lin (1984), iron from Brown et al. (2000), $H_2O$ ice from Ahrens and Johnson (1995).

anhydrite did occur in the sample. Chen et al. (1994) addressed the effect of reducing iron, and Yang and Ahrens (1998) and Gupta et al. (2001) measured velocity profiles of shocked porous anhydrite and employed the entropy criterion to model vaporization of material under the shock compression process. The estimated pressures for incipient and the complete vaporization along the Hugoniot of anhydrite are 32.5 and 122 GPa, respectively. According to these results on anhydrite, vaporization will occur to a lesser degree at pressures up to about 60 GPa and it proceeds abruptly above the critical shock pressure. Another thermodynamic calculation for non-porous anhydrite (Ivanov et al., 2004) gives estimates for melting at 80–90 GPa, incipient decomposition at 60–70 GPa, and equilibrated decomposition at 100–110 GPa, respectively. For calcite decarbonation, the produced CaO has been known to be highly reactive to revert to $CaCO_3$ during shock pressure release (Agrinier et al., 2001). Similarly, anhydrite decomposition may have reverted to $CaSO_4$ on pressure release. Vaporization of magnesium sulfate follows a similar path, and would occur at a relatively lower temperature due to the stability difference at ambient pressure.

It has been generally recognized that most sulfates, which may be present on the surface of Mars, can be hydrated easily to retain moisture. The present experiments have indicated that the dehydration can also easily occur in the propagation process of shock waves generated by impacts. The properties of sulfates and sulfate hydrates imply that the total amount of water as a volatile substance would be kept almost constant even if Mars is subjected to heavy bombardment. This further suggests that a large amount of water in the liquid form was not present on Mars except at the time of Mars formation and that the early Mars had an atmosphere and volatiles near the subsurface. These hydration and dehydration reactions may have played a key role as a resurfacing process on Mars as well as a possible process for life on Mars (Squyres et al., 2004).

## ACKNOWLEDGMENTS

DTA/TG analysis was performed at Shimadzu Analysis Center. Comments and suggestions by C. Koeberl and an anonymous reviewer helped us to improve the draft, and the authors thank W.U. Reimold for editing. This work and the stay of F.Z. in NIMS were supported by the Grant-in-Aid for Scientific Research JSPS (No. 18204051).

## REFERENCES

Abriel W., Reisdorf K. and Pannetier J. (1990) Dehydration reactions of gypsum: a neutron and x-ray diffraction study. *J. Solid State Chem.* **85**, 23–30.

Agrinier P., Deutsch A., Scharer U. and Martinez I. (2001) Fast back-reactions of shock-released $CO_2$ from carbonates: an experimental approach. *Geochim. Cosmochim. Acta* **65**, 2615–2632.

Ahrens, T. J. and M. L. Johnson (1995) Shock wave data for minerals. In *Mineral Physics & Crystallography. A Handbook of Physical Constants* (ed. T. J. Ahrens), American Geophysical Union Washington, DC, pp. 143–184.

Alvarez L. W., Alvarez W., Asaro F. and Michel H. V. (1980) Extraterrestrial cause for the Cretaceous/Tertiary extinction. *Science* **208**, 1095–1108.

Anderson, W. W. and Ahrens, T. J. (1998) Shock wave equation of state of chondritic meteorites. In *Shock Compression of Condensed Matter—1997* (eds. S. C. Schmidt, D. P. Dandekar and J. W. Forbes). American Institute of Physics, New York, pp. 115–118.

Bonello, G., Berthet, P. and d'Hendecout, L. (2005) Identification of magnesium sulfate hydration state derived from NIR refractance spectroscopy. In *Lunar and Planetary Science*, vol. XXXVI. Abstract #1996, Lunar and Planetary Institute, Houston (CD-ROM).

Brett R. (1992) The Cretaceous–Tertiary extinction: a lethal mechanism involving anhydrite target rocks. *Geochim. Cosmochim. Acta* **56**, 3603–3606.

Brown J. W., Fritz J. N. and Hixon R. S. (2000) Hugoniot data for iron. *J. Appl. Phys.* **88**, 5496–5498.

Burgess R., Wright I. P. and Pillinger C. P. (1991) Determination of sulphur-bearing components in C1 and C2 carbonaceous chondrites by stepped combustion. *Meteoritics* **26**, 55–64.

Calleri M., Gavetti A., Ivaldi G. and Rubbo M. (1984) Synthetic epsomite, $MgSO_4 \cdot 7H_2O$: Absolute configuration and surface features of the complementary {111} forms. *Acta Cryst.* **B40**, 218–222.

Chen G., Tyburczy J. A. and Ahrens T. J. (1994) Shock-induced devolatilization of calcium sulfate and implications for K–T extinctions. *Earth Planet. Sci. Lett.* **128**, 615–628.

Chipera S. J. and Vaniman D. T. (2007) Experimental stability of magnesium sulfate hydrates that may present on Mars. *Geochim. Cosmochim. Acta* **71**, 241–250.

Chou I.-M. and Seal, II, R. R. (2003) Determination of epsomite–hexahydrite equilibria by the humidity-buffer technique at 0.1 MPa with implications for phase equilibria in the system $MgSO_4$–$H_2O$. *Astrobiology* **3**, 619–630.

Christensen, P. R. and Moore, H. J. (1992) The martian surface layer. In *Mars* (eds. H. H. Kieffer, B. M. Jakovsky, C. W. Snyder and M. S. Matthews). University of Arizona Press, Tucson, pp. 686–729.

Ciesla F. J., Lauretta D. S., Cohen B. A. and Hood L. L. (2003) A nebula origin for chondritic fine-grained phyllosilicates. *Science* **299**, 549–552.

Clark B. C., Baird A. K., Weldon R. J., Tsukasaki D. M., Schnabel L. and Candelaria M. P. (1982) Chemical composition of Martian fines. *J. Geophys. Res.* **87**, 8395–8403.

DeCarli, P. S., Bowden, E., Jones, A. P. and Price, G. D. (2002). Laboratory impact experiments versus natural impact events. In *Catastrophic Events and Mass Extinctions: Impacts and Beyond* (eds. C. Koeberl and K. MacLeod). Geol. Soc. Amer. Spec. Pap., **356**, pp. 595–605.

Farquhar J., Savarino J., Jackson T. L. and Thiemens M. H. (2000) Evidence of atmospheric sulphur in the martian regolith from sulphur isotopes in meteorites. *Nature* **404**, 50–52.

Fritz J., Artemieva N. and Greshake A. (2005) Ejection of Marian meteorites. *Meteoritics Planet. Sci.* **40**, 1393–1411.

Gellert R., Rieder R., Anderson R. C., Brückner J., Clark B. C., Dreibus G., Economou T., Klingelhöfer G., Lugmair G. W., Ming D. W., Squyres S. W., d'Uston C., Wänke H., Yen A. and Zipfel J. (2004) Chemistry of rocks and soils in Gusev crater from the alpha particle X-ray spectrometer. *Science* **305**, 829–832.

Gendrin A., Mangold N., Bibring J.-P., Langevin Y., Gondet B., Poulet F., Bonello G., Quantin C., Mustard J., Arvidson R. and LeMoúelic S. (2005) Sulfates in martian layered terrains: the OMEGA/Mars Express view. *Science* **307**, 1587–1591.

Gounelle M. and Zolensky M. E. (2001) A terrestrial origin for sulfate veins in CI1 chondrites. *Meteoritics Planet. Sci.* **36**, 1321–1329.

Gupta S. C., Ahrens T. J. and Yang W. (2001) Shock-inducted vaporization of anhydrite and global cooling from the K/T impact. *Earth Planet. Sci. Lett.* **188**, 399–412.

Hawthorne F. C., Groat L. A., Raudsepp M. and Ercit T. S. (1987) Kieserite, $Mg(SO_4)(H_2O)$, a titanite-group mineral. *Neues. Jahrb. Min.* **157**, 121–132.

Hawthorne, F. C., Krivovichev, S. V. and Burns, P. C. (2000) The crystal chemistry of sulfate minerals. In *Sulfate Minerals: Crystallography, Geochemistry, and Environmental Significance, Reviews in Mineralogy and Geochemistry* (eds. C. N. Alpers, J. L. Jambor and D. K. Nordstrom). Mineralogical Society of America Washington, DC, pp. 1–112.

Ivanov, B. A., Langenhorst, F., Deutsch, A. and Hornemann, U. (2002) How strong was the impact-induced $CO_2$ degassing in the K/T event? Numerical modeling of laboratory experiments. In *Catastrophic events and Mass Extinctions: Impact and beyond* (eds. C. Koeberl and K. G. MacLeod). Geol. Soc. Amer. Spec. Pap., **356**, pp. 587–594.

Ivanov, B. A., Langenhorst, F., Deutsch, A. and Hornemann, U. (2004) Anhydrite EOS and phase diagram in relation to shock decomposition. In *Lunar and Planetary Science*, vol. XXXV. Abstract #1489, Lunar and Planatary Institute, Houston (CD-ROM).

Knauth L. P., Burt D. M. and Wohletz K. H. (2005) Impact origin of sediments at the Opportunity landing site on Mars. *Nature* **438**, 1123–1128.

Kondo K.-I., Sawaoka A. and Saito S. (1977) Magnetoflyer method for measuring gas-gun projectile velocities. *Rev. Sci. Instrum.* **48**, 1581–1582.

Langenhorst, F., Boustie, M., Deutsch, A., Hornemann, U., Matignon, Ch., Migault, A. and J. P. Romain (2003) Experimental techniques for the simulation of shock metamorphism: a case study on calcite. In *High-pressure Shock Compression of Solids. V: Shock Chemistry with Applications to Meteorite Impacts* (eds. L. Davison, Y. Horie and T. Sekine). Springer, New York, pp. 1–27.

Langevin Y., Poulet F., Bibring J.-P. and Gondet B. (2005) Sulfates in the north polar region of Mars detected by OMEGA/Mars Express. *Science* **307**, 1584–1586.

Leshin L. A., Rubin A. E. and McKeegan K. D. (1997) The oxygen isotopic composition of olivine and pyroxene from CI chondrites. *Geochim. Cosmochim. Acta* **61**, 835–845.

Lin W.-Z. (1984) Shock compression of Jilin meteorite and pyrolite model. *Chin. J. Space Sci.* **4**, 338–346.

McConnell J. D. C., Astill D. M. and Hall P. L. (1987) The pressure dependence of the dehydration of gypsum to bassanite. *Min. Mag.* **51**, 453–457.

Nyquist L. E., Boqard D. D., Shin C.-Y., Greshake A., Stöffler D. and Eugster O. (2001) Ages and geological histories of Martian meteorites. *Space Sci. Rev.* **96**, 105–164.

Paulik J., Paulik F. and Arnold M. (1981) Dehydration of magnesium sulfate heptahydrate investigated by quasi isothermal–quasi isobaric TG. *Thermochim. Acta* **50**, 105–110.

Pierazzo E., Vickery A. M. and Melosh H. J. (2001) A reevaluation of impact melt production. *Icarus* **127**, 408–423.

Pope K. O., Baines K. H., Ocampo A. C. and Ivanov B. A. (1997) Energy, volatile production, and climatic effects of the Chicxulub Cretaceous/tertiary impact. *J. Geophys. Res.* **102**, 21645–21664.

Richardson S. M. (1978) Vein formation in the C1 carbonaceous chondrites. *Meteoritics* **13**, 141–159.

Rowe J. J., Morey G. W. and Silber C. C. (1967) The ternary system $K_2SO_4$–$MgSO_4$–$CaSO_4$. *J. Inorg. Nucl. Chem.* **29**, 929–942.

Sekine T. (1997) Shock wave chemical synthesis. *Eur. J. Solid State Inorg. Chem.* **34**, 823–833.

Sigurdsson H., D'Hondt S. and Carey S. (1992) The impact of the Cretaceous/tertiary bolide on evaporite terrane and generation of major sulfic acid aerosol. *Earth Planet. Sci. Lett.* **109**, 543–559.

Simakov G. V., Pavlovskiy N. M., Kalashnikov N. G. and Trunin R. F. (1974) Shock compressibility of twelve minerals. *Izv. Phys. Solid Earth* **8**, 488–492.

Skála, R., Hörz, F. P. and Langenhorst, F. (2005) Experimentally shock-loaded anhydrite: Unit-cell dimensions, microstrain and domain size from X-ray powder diffraction. In *Large Meteorite Impacts III* (eds. T. Kenkmann, F. Horz, A. Deutsch). *Geol. Soc. Am. Spec. Pap.* **384**, pp. 413–425.

Squyres S. W., Grotzinger J. P., Arvidson R. E., Bell J. F., Calvin W., Christensen P. R., Clark B. C., Crisp J. A., Farrand W. H., Herkenhöff K. E., Johnson J. R., Klingelhöfer G., Knoll A. H., McLennan S. M., McSween H. Y., Morris R. V., Rice J. W., Rieder R. and Soderblom L. A. (2004) In situ evidence for an ancient aqueous environment at Meridiani Planum, Mars. *Science* **306**, 1709–1714.

Tomeoka K., Yamahana Y. and Sekine T. (1999) Experimental shock metamorphism of the Murchison CM carbonaceous chondrite. *Geochim. Cosmochim. Acta* **63**, 3683–3703.

Tonui E. K., Zolensky M. E., Lipschutz M. E., Wang M. and Nakamura T. (2003) Yamato 86029: Aqueously altered and thermally metamorphosed CI-like chondrite with unusual textures. *Meteoritics Planet. Sci.* **38**, 269–292.

Vaniman D. T. and Chipera S. J. (2006) Transformations of Mg- and Ca-sulfate hydrates in Mars legolith. *Am. Miner.* **91**, 1628–1642.

Vaniman D. T., Bish D. L., Chipera S. J., Fialips C. I., Carey J. W. and Feldman W. C. (2004) Magnesium sulfate salts and the history of water on Mars. *Nature* **431**, 663–665.

Yang W. and Ahrens T. J. (1998) Shock vaporization of anhydrite and global effects of the K/T bolide. *Earth Planet. Sci. Lett.* **156**, 125–140.

Zalkin A., Ruben H. and Templeton D. H. (1964) The crystal structure and hydrogen bonding of magnesium sulfate hexahydrite. *Acta Cryst.* **17**, 235–240.

*Associate editor:* W. Uwe Reimold